

Original paper

Sulfide anomaly related to cymrite–quartz schist of the Kalugeri area, Pelagonian massif, Republic of North Macedonia

Marko BERMANEC^{1*}, Nikita V. CHUKANOV², Dmitry A. VARLAMOV³, Ana RAJAČIĆ⁴,
Simeon JANČEV⁴, Vera N. ERMOLAEVA³

¹ Institute of Geological Sciences, Universität Bern, Baltzerstrasse 1+3, 3012 Bern, Switzerland; marko.bermanec@gmail.com

² Institute of Chemical Physics Problems, Russian Academy of Sciences, Chernogolovka, Moscow region, 142432 Russia

³ Institute of Experimental Mineralogy, Russian Academy of Sciences, Chernogolovka, Moscow Region, 142432 Russia

⁴ Faculty of Technology and Metallurgy, Saints Cyril and Methodius University, Ruger Boskovic 16, 1000 Skopje, Republic of North Macedonia

*Corresponding author



A specific feature of a major part of regional metamorphosed metasomatic ores of the Nežilovo area, Pelagonian massif, Republic of North Macedonia is the occurrence of chalcophile elements (Zn, Pb, Sb, Cu, and As) in oxides and oxyalts whereas sulfides and sulfosalts are absent. This paper describes anomalous sulfide-bearing mineral assemblage discovered in small, localized outcrops at the Kalugeri locality belonging to the Nežilovo group of ore occurrences. Based on the data on mineral assemblages and associations, a four stage model is proposed. Pressures of the first stage was estimated to be above 20 kbar using barometry on Ba-rich first generation of phengite and temperatures above 530 °C were estimated by Zr in rutile thermometer. During this stage, sulfide mineralization still occurs with crystallization of sphalerite and galena. In the second stage occurring above 500 °C and above 10 kbar, the first generation of cymrite crystallized showing that barium was present in the system in excess compared to sulfur. The third stage was dominated by Zn-rich phengite, baryte–anglesite solid solution and cerussite formation at temperatures between 500 and 350 °C and pressures between 7.1 and 4 kbar. The final stage of formation is characterized by crystallization of the second generation of cymrite below 350 °C. It is concluded that sulfide-free ores of the Nežilovo type could form as a result of transformation of initial sulfide ores at low-PT conditions and a high barium activity.

Keywords: sulfide relicts, cymrite, metasomatism, regional metamorphism, Nežilovo area, Pelagonian massif

Received: 9 May 2023; **accepted:** 15 December 2023; **handling editor:** J. Sejkora

1. Introduction

The Mixed Series metamorphic complex of the Pelagonian massif (Fig. 1) situated near the Nežilovo village, Republic of North Macedonia (about 41°41' N, 21°25' E) is composed mainly of albite gneisses hosting bodies of meta-rhyolites and lenses of dolomitic marbles. According to Stojanov (1960), metamorphic rocks of Mixed Series are the products of regional metamorphism of marine sediments enriched in alkaline elements.

Ore bodies of the Nežilovo area are mainly concordant with the host rocks (Jančev 1975a) and have a synchronous evolution with one another. Zones enriched in chalcophile elements (S, As, Sb, Zn, Cu, Pb) are enclosed in dolomitic marbles. The marbles are partly metasomatically replaced by baryte schists forming lenses and layers up to 150 m long, with a thickness up to 10 m (Barić and Ivanov 1960; Ivanov and Jančev 1976; Jančev 1984, 1994; Bermanec et al. 1996; Chukanov et al. 2015). These are leucocratic rocks char-

acterized by fine- or medium-grained structure and schistose texture.

Metamorphosed metasomatic rocks of the Mixed Series are very complex and presented by unusual mineral assemblages in which baryte, dolomite, cymrite, tilasite, quartz, various Zn-bearing silicates (diverse amphiboles, micas, and talc), locally albite, potassium feldspar, clinopyroxene, hematite, and/or Zn-spinels (gahnite and franklinite) are the major rock-forming minerals. The accessory mineralization of these metasomatic rocks and ores includes over 50 mineral species with five of them (nežilovite, piemontite-(Pb), ferricoronadite, zincohögbomite-2N6S and zincovelesite-6N6S) being newly described (Barić 1960; Barić and Ivanov 1960; Jančev 1975b, 1994, 1998; Bermanec et al. 1994, 1996; Armbruster et al. 1998; Holtstam et al. 2001; Jančev et al. 2016, 2021; Chukanov et al. 2012, 2015, 2016, 2018a, b, 2019, 2020a, b; Ermolaeva et al. 2016, 2019a, b; Varlamov et al. 2018, 2019, 2021). Post-magmatic fluids related to meta-rhyolites are considered as a possible

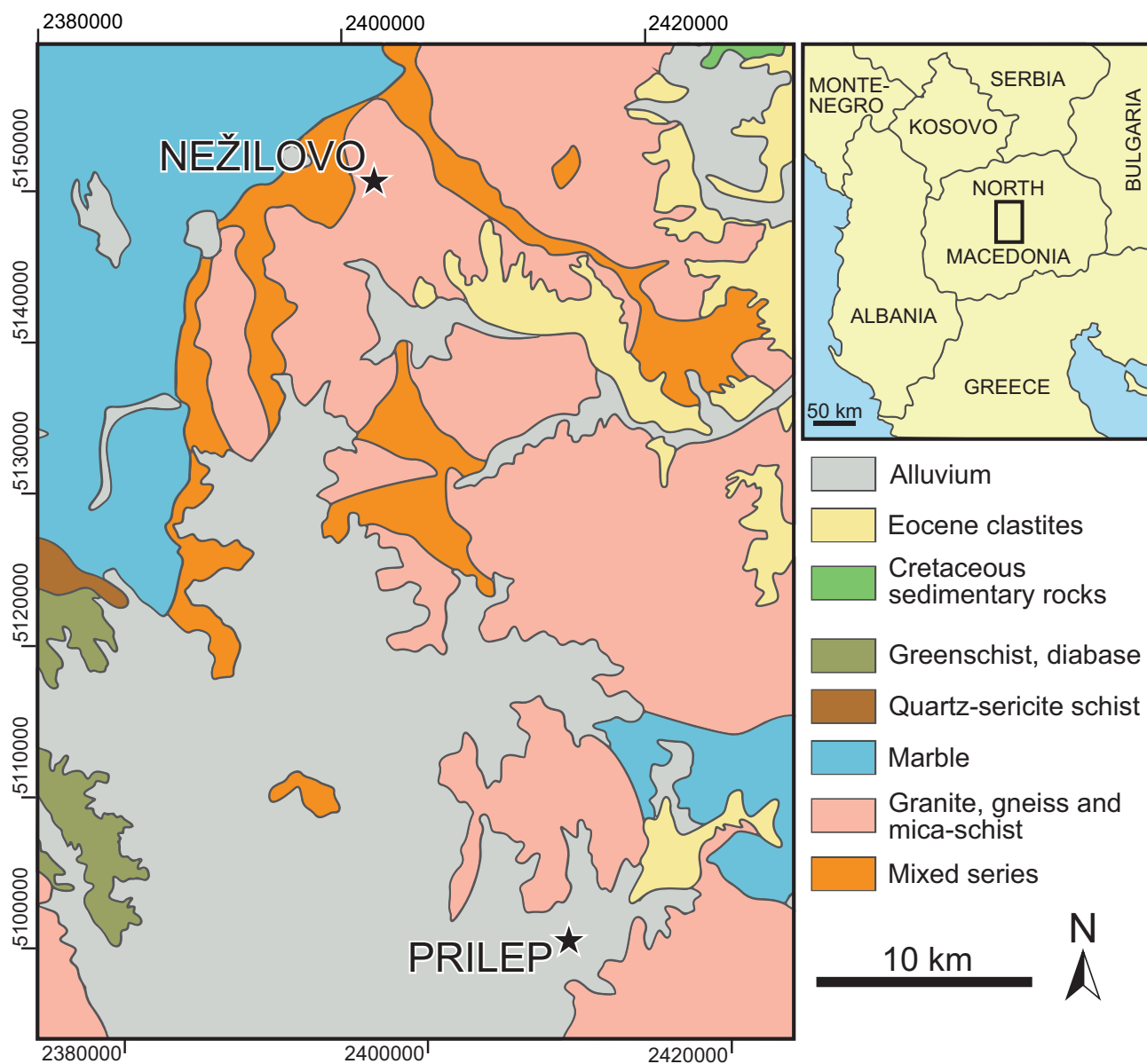


Fig. 1. Geological map of the Nežilovo area adapted from Bermanec et al. (2021).

source of some specific, ore and rare elements (Pb, Zn, Sb, As, Cu, Ba, REE etc.) (Jančev 1998). These rocks formed under highly oxidizing conditions and at a high activity of barium which is an effective precipitant of sulfur (Blount 1977). As a result, a specific feature of the major part of these metasomatic assemblages is the occurrence of chalcophile elements (Zn, Cu, Pb, Sb, As) in oxygen-bearing minerals (oxides and oxysalts) whereas sulfides are absent.

Based on mutual phase relations between Ba-bearing minerals (baryte, cymrite, and hyalophane), it was concluded that their crystallization had a continuous character ending with a low-temperature hydrothermal stage (Jančev 1975a). Coarse-grained cymrite forms individuals up to 2 cm across in cymrite-quartz schists in

which other barium minerals, rutile, titanite, occasionally sulfides (pyrite, galena, and sphalerite) and allanite-(Ce) are the accessory components.

2. Materials and methods

2.1. Optical petrography

Samples were cut and section surfaces were polished with diamond pastes 6–3–1 μm on cloth to obtain a mirror finish. Places of interest were selected by back-scattered electron (BSE) imaging to identify locations suitable for in-situ analysis of mineral composition by electron-probe instruments (see below), with scratch-free surface, no

visible inclusions, and with well-defined mineral grain boundaries.

2.2. In-situ mineral chemistry

In situ microanalysis and backscatter imaging were done in a Tescan Vega-II XMU scanning electron microscope (SEM) instrument equipped with an Oxford Instruments INCA Energy 450 energy-dispersive spectrometer (EDS) Si(Li) detector and an INCA Wave 700 inclined wavelength-dispersive spectrometer (WDS), as well as on CamScan MV2300 and Vega TS 5130MM SEM instruments each with an EDS detector. Backscatter and secondary electron imaging was done with a YAG-scintillator detector. The EDS method of analysis was applied to obtain more detailed information on the mineral assemblage and more statistically representative data for variations of chemical compositions of minerals. WDS method was used to control the correctness of the EDS data and for the detection of minor and trace elements. In all cases, there was an agreement between EDS and WDS data in the limits of chemical nonhomogeneity of minerals.

Acquisition time for EDS spectra was 100 s (dead time kept at minimum 20 %), and for each element measured by WDS it was 20 s. The sample-to-detector distance is 25 mm. The analyses were performed at an accelerating voltage 20 kV. Current of the absorbed electrons on a reference sample of cobalt was 195–210 pA (20 nA in WDS mode), and on the studied polished samples – from 150 to 400 pA (10–40 nA in WDS mode) depending on a microrelief, structure and composition of samples. The size of an electronic “spot” on a surface of a sample vary at range 157–180 nanometers (300–320 nm in WDS mode), in a scanning mode – to 60 nanometers, the zone of “excitation” can reach 4–5 micrometers (depending on a microrelief, structure, composition and density of samples).

The Tescan Vega II XMU instrument was internally calibrated against natural and synthetic mineral substances and pure metals: SiO₂ (*Kα*) for O, MgF₂ (*Kα*) for F, NaCl (*Kα*) for Cl, synthetic FeS₂ (*Kα*) for S, synthetic LaPO₄ (*Kα*) for P, albite (*Kα*) for Na, orthoclase (*Kα*) for K, MgO (*Kα*) for Mg, wollastonite (*Kα*) for Ca, synthetic Al₂O₃ (*Kα*) for Al, pure Mn (*Kα* and *Lα*) for Mn, pure Fe (*Kα* and *Lα*) for Fe, pure copper (*Kα* and *Lα*) for Cu, pure Zn (*Kα* and *Lα*) for Zn, pure Si (*Kα*) for Si, pure Ti (*Kα*) for Ti, pure Zr (*Lα*) for Zr, pure Hf (*Lα* and *Mα*) for Hf, pure Nb (*Lα*) for Nb, pure W (*Lα* and *Mα*) for W, BaF₂ (*Lα*) for Ba, PbTe (*Lα* and *Mα*) for Pb, synthetic InAs (*Kα* and *Lα*) for As, and synthetic REE(PO₄) (*Lα* and *Mα*) for corresponding rare-earth elements. Calculations of results of the X-ray spectral microanalysis were carried out by means of a software package of INCA Microanalysis

Suite 4.15 (version 18d+SP4) with an option of the accounting of possible matrix effects for WDS analysis.

2.3. Fourier-transform infrared (FTIR) spectroscopy

In order to obtain infrared (IR) absorption spectra, powdered samples were mixed with KBr predried at 120 °C, formed into a transparent pellet by pressurizing the mix at 10 tons in a hydraulic jack for 3 min, and analyzed using an ALPHA FTIR spectrometer (Bruker Optics) with a resolution of 4 cm⁻¹. A total of sixteen scans were obtained for each spectrum. The IR spectrum of a pellet of pure KBr was used as a reference blank.

3. Results

The sulfide-bearing mineral assemblage consists of cymrite substituting baryte (up to 70 vol. % of the rock), quartz (~10 vol. %), micas (5–7 vol. %), galena partly replaced by Ba-bearing anglesite and Pb-bearing baryte (5–7 vol. %), and Pb-free baryte (~3 vol. %). Accessory mineralization is rather diverse and includes titanite, rutile, zircon, a crichtonite group mineral (Zr-free analogue of lindsleyite), willemite, sphalerite, Ag-bearing covellite, and cerussite (Fig. 2).

The order of mineral formation in the sulfide-bearing assemblage of the Kalugeri locality is presented in Fig. 3. Titanium minerals, zircon, galena, sphalerite, Ba-bearing and Zn-bearing phengite, quartz, and relics of Pb-free baryte of the first generation belong to the earliest paragenesis. Relict sphalerite grains are preserved mainly in ‘capsules’ composed of anglesite and quartz (Fig. 2 b, c). At the second stage of mineral formation, partial substitution of galena with Pb, Ba-sulfates and partial decomposition of sphalerite accompanied by the crystallization of willemite took place. Decomposition of galena was accompanied by the exsolution of copper and formation of Ag-rich covellite (Figs. 2 f, h; Tab. 1). This process proceeded before or simultaneously with cymrite crystallization. The formation of sulfides at this stage was inhibited because of a high Ba activity. At the third stage, most of Pb-free baryte was substituted with cymrite, and fine-grained aggregates of Pb, Ba-sulfates and cerussite were formed. Unlike most other ore occurrences of this area, at the Kalugeri locality only a partial substitution of sulfides with oxygen-bearing minerals took place.

Three generations of baryte and two generations of anglesite are observed. Pb-free baryte of the first generation forms fine-grained aggregates and is a relic of baryte schist (Fig. 2d). Baryte of the second generation contains Pb and forms partial or complete pseudomorphs after galena with low-barium anglesite of the first generation

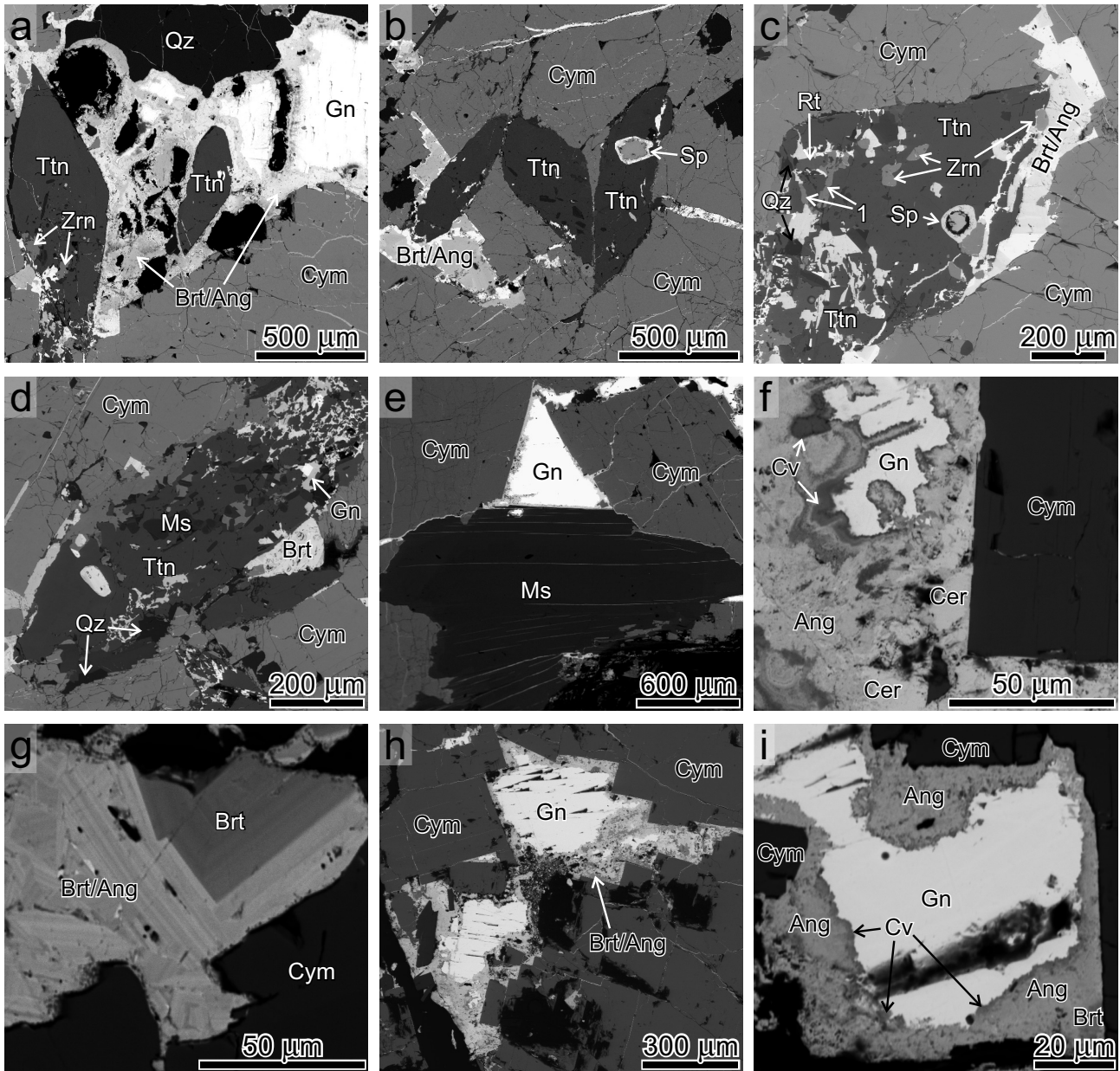


Fig. 2. SEM-BSE images demonstrating mineral assemblages of the first generation at the Kalugeri occurrence. **a, b, c, d** – Euhedral to subhedral grains of typical lenticular titanite (Ttn) with inclusions of a crichtonite-group mineral, rutile (Rt), zircon (Zrn), baryte (Brt) of the first generation, Zn-free phengite (Ms) of the first generation, quartz (Qz), and sphalerite (Sp) (as inclusions in anglesite±quartz), in association with cymrite (Cym) and minerals of the baryte-anglesite (Brt/Ang) solid-solution series replacing galena (Gn); **e** – Phengite of the second generation in contact with cymrite and galena; **f** – euhedral cymrite crystal in contact with fine-grained aggregate of cerussite and anglesite of the second generation, in association with relic of galena surrounded by covellite (Cv); **g** – fine-grained aggregate of baryte and anglesite of the second generation in contact with cymrite and quartz; **h, i** – Partial pseudomorphs of Pb-bearing baryte and Ba-bearing anglesite of the first generation after euhedral and subhedral galena crystals in cymrite. The abbreviations of mineral names are given in accordance with IMA–CNMNC approved mineral symbols (Warr 2021). The symbol 1* denotes a crichtonite-group mineral.

(Fig. 2c, h, i). Ba-rich anglesite of the second generation, Pb-bearing baryte of the third generation, and cerussite constitute late, fine-grained aggregates filling cavities with euhedral cymrite crystals (Fig. 2f, g). The representative EMPA analyses of minerals of this paragenesis are given in Tab. 2.

Di-octahedral micas of the first generation contain significant amounts of Zn and form anhedral inclusions

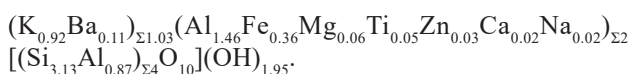
in titanite (Fig. 2d). Micas of the second generation are zinc-free (Fig. 2e). Cymrite which is the major mineral in this assemblage is potassium rich with K_2O reaching 1.14 wt. %. Some cymrite contains detectable amounts of sodium and calcium (Na_2O up to 0.31 wt. % and CaO up to 0.21 wt. %) (Tab. 3).

Inner zones of the largest titanite crystals are enriched in Al and Fe (Al_2O_3 and Fe_2O_3 up to 1.3 wt. %)

Tab. 2. Main element oxide contents in selected Ba,Pb sulfates and cerussite by EDS and WDS, in wt. %.

Component	Baryte			Anglesite		Cerussite
SO ₃	33.42	32.62	30.00	29.90	28.49	b.d.l.
SrO	b.d.l.	b.d.l.	b.d.l.	0.06*	0.22*	b.d.l.
BaO	66.38	56.15	35.36	21.84	0.56	b.d.l.
PbO	1.18	12.01	35.33	46.92	70.61	81.91
Total	100.98	100.78	100.69	98.72	99.88	81.91
Formula coefficients based on S 1 <i>apfu</i> for baryte and anglesite and 1 cation <i>pfu</i> for cerussite						
S	1.00	1.00	1.00	1.00	1.00	0
Sr	0	0	0	0	0.01	0
Ba	1.04	0.90	0.62	0.38	0.01	0
Pb	0.01	0.13	0.42	0.56	0.89	1.00

Note: "b.d.l." means "below detection limit".



Analysis 3 with Si > 3.5 atoms per formula unit (*apfu*) represents Fe- and Zn-rich celadonite (phengite of the first generation forming inclusions in titanite). The analysis 4 represents Ba- and Fe-bearing muscovite which is confined to cymrite aggregates (phengite of the second generation).

IR spectrum of cymrite (Fig. 5) shows that this mineral is presented by the monoclinic modification. Cymrite

Tab. 3. Main element oxide contents in selected Ti- and Zr-containing minerals by EDS and WDS, in wt. %.

Component	Cymrite		Phengite (celadonite)	Phengite (muscovite)		Willemite
Na ₂ O	b.d.l.	b.d.l.	0.43	0.13	0.19	b.d.l.
K ₂ O	1.14	0.11	11.37	10.05	9.07	b.d.l.
CaO	0.04	0.21	0.09	0.25	0.08	b.d.l.
BaO	38.53	39.61	0.55	3.82	5.81	b.d.l.
MgO	b.d.l.	b.d.l.	2.73	0.60	0.87	b.d.l.
MnO	b.d.l.	b.d.l.	0.16	b.d.l.	0.17	b.d.l.
FeO	b.d.l.	b.d.l.	3.93	6.69	6.12	b.d.l.
ZnO	b.d.l.	b.d.l.	3.02	0.62	b.d.l.	73.73
Al ₂ O ₃	25.32	25.55	21.09	27.35	28.69	b.d.l.
SiO ₂	33.01	29.92	52.01	43.94	42.09	25.96
TiO ₂	b.d.l.	b.d.l.	0.43	0.76	1.53	b.d.l.
F	b.d.l.	b.d.l.	0.45	0.20	0.17	b.d.l.
-O=F	0	0	0.19	0.08	0.07	0
Total	98.04	95.40	96.07	94.33	94.86	99.69
Formula coefficients based on 4(Si+Al) <i>apfu</i> for cymrite, 6 cations except K and Ba for phengite, 1 Si <i>apfu</i> for willemite						
Na	0	0	0.06	0.02	0.03	0
K	0.09	0.01	0.99	0.92	0.83	0
Ca	0	0.02	0.01	0.02	0.01	0
Ba	0.96	1.03	0.01	0.11	0.16	0
Mg	0	0	0.28	0.06	0.09	0
Mn	0	0	0.01	0	0.01	0
Fe	0	0	0.20	0.36	0.33	0
Zn	0	0	0.15	0.03	0	2.10
Al	1.90	2.01	1.70	2.33	2.43	0
Si	2.10	1.99	3.57	3.13	3.03	1.00
Ti	0	0	0.02	0.05	0.08	0
F	0	0	0.10	0.05	0.04	0

individuals are anhedral at contacts with all minerals except cerussite and members of the anglesite–baryte solid-solution series forming late fine-grained aggregates outside the pseudomorphs after galena (Fig 2 h, i).

4. Discussion

Nežilovo belongs to the area characterized by complex poly-phase regional metamorphic events (Ivanov 1961; Most 2003; Bermanec et al. 2021) further complicated due to the formation of cross-cutting veins and dikes, such as pegmatites described in Boev and Bermanec (2021). At the early stages, oceanic sedimentary rocks were in contact with extrusions of alkali-granitic lavas. At these contacts, complex ores of metasomatic nature were formed, however any contact metamorphic rocks were subsequently regionally metamorphosed which lead to metamorphic overprint of older metamorphic events. Majer and Mason (1983) describe some characteristics of an eclogite facies such as an omphacite association in some samples and interpret garnets as relicts of the previous meta-sediments. These high-grade regional metamorphic rocks are the main setting of the central part of the Pelagonian Massif (Stojanov 1968; Mountrakis 1984).

In the next stage, the whole geological complex underwent high-grade regional metamorphism at high-pressure epidote–amphibolite facies conditions peaking in the Cretaceous period which was retrograded towards greenschist conditions.

Sulfide-free mineral assemblages with high contents of chalcophile elements are quite rare. The most well-known occurrences of this type are Franklin and Sterling Hill Fe–Zn deposits in New Jersey, USA (Palache 1929a,b; Tarr 1929; Wilkerson 1962; Peck et al. 2009), Långban, Nordmark (including Jakobsberg) and Pajsberg (including Harstigen)

Fe–Mn deposits in the Bergslagen ore province, Värmland, Sweden (Palache 1929a; Nysten et al. 1999), Mendip Hills, England (Turner and Rumsey 2010), and some kinds of ores of the Kombat deposit in Namibia (Innes and Chaplin 1986; Dunn 1991). At the zinc deposits of New Jersey (Franklin and Sterling Hill), the chief primary zinc mineral is sphalerite which is associated with varying amounts of other sulfides including pyrite or marcasite, galena, and chalcopyrite. Tarr (1929) supposed that oxidation of sphalerite resulted in the formation of Zn-bearing oxides and silicates, including franklinite, zincite, willemitte, and tephroite. Pb-bearing silicates occurring at these deposits, including epidote-(Pb) and roeblingite (Palache 1937), could be products of galena oxidation and subsequent reactions with hot fluids. In the sulfide anomaly of the Kalugeri occurrence, partial substitution of sulfides with oxygen-bearing minerals is observed. This observation may give a key for the understanding the mechanisms of formation of ores of such type.

The Zr-in-rutile geothermometer (Watson et al. 2006) was used for the estimation of the pressure conditions of the first stage of mineralization. The geothermometer gave results between 535 and 613 °C for the values of Zr content in the core of rutile crystals (about 120 ppm). The Zr concentration decreases from core to rim and

at the rim it drops below limit of detection (*i.e.* below 60 ppm). For this concentration, the temperature could not have been higher than 564 °C. However, since the Zr content at the rims is below LOD the temperature might have been even lower than 493 °C which is the lower limit of the calculated temperature interval for 60 ppm Zr.

To determine the pressure conditions more precisely, an empirical phengite geobarometer was used (Kam-

Tab. 4. Main element oxide contents in selected silicates (except titanite) by EDS and WDS, in wt. %.

Component	Crichtonite-group mineral	Rutile	Titanite	Zircon		
K ₂ O	b.d.l.	b.d.l.	b.d.l.	0.12	0.14	b.d.l.
Na ₂ O	b.d.l.	b.d.l.	b.d.l.	b.d.l.	0.12	b.d.l.
CaO	0.25	b.d.l.	b.d.l.	28.07	27.91	0.13*
MgO	b.d.l.	b.d.l.	b.d.l.	b.d.l.	0.10	b.d.l.
TiO ₂	67.20	66.63	98.83	39.68	40.37	0.31*
Al ₂ O ₃	b.d.l.	b.d.l.	b.d.l.	1.22	1.17	0.29
SiO ₂	b.d.l.	b.d.l.	b.d.l.	29.71	28.91	31.30
MnO	1.72	1.56	b.d.l.	0.03	b.d.l.	b.d.l.
FeO	20.08	20.88	1.58	0.43	0.09	b.d.l.
ZnO	1.77	1.86	b.d.l.	0.36	b.d.l.	b.d.l.
SrO	1.25*	0.90*	0.62*	b.d.l.	b.d.l.	b.d.l.
Y ₂ O ₃	1.08	1.66	b.d.l.	b.d.l.	b.d.l.	b.d.l.
BaO	6.18	6.84	b.d.l.	b.d.l.	b.d.l.	b.d.l.
PbO	b.d.l.	1.40	b.d.l.	b.d.l.	b.d.l.	b.d.l.
ZrO ₂	b.d.l.	b.d.l.	b.d.l.	b.d.l.	b.d.l.	65.65
HfO ₂	b.d.l.	b.d.l.	b.d.l.	b.d.l.	b.d.l.	1.59
Nb ₂ O ₅	b.d.l.	b.d.l.	0.43*	b.d.l.	b.d.l.	b.d.l.
Nd ₂ O ₃	b.d.l.	b.d.l.	b.d.l.	b.d.l.	b.d.l.	0.08
UO ₃	b.d.l.	b.d.l.	b.d.l.	b.d.l.	b.d.l.	0.67
F	b.d.l.	b.d.l.	b.d.l.	0.77	0.19	b.d.l.
–O=F	0	0	0	0.32	0.08	0
Total	99.53	101.73	101.46	100.07	98.92	100.02
Formula coefficients based on 38 O for crichtonite-group mineral, 1 cation pfu for rutile, 1(Si+Al) pfu for titanite and zircon						
K	0	0	0	0	0.01	0
Na	0	0	0	0	0.01	0
Ca	0.08	0	0	0.97	0.99	0
Mg	0	0	0	0	0.01	0
Ti	14.42	14.26	0.98	0.96	1.00	0.01
Al	0	0	0	0.05	0.05	0.01
Si	0	0	0	0.95	0.95	0.99
Mn	0.41	0.38	0	0	0	0
Fe	4.79	4.97	0.02	0.01	0	0
Zn	0.37	0.39	0	0.01	0	0
Sr	0.20	0.15	0	0	0	0
Y	0.16	0.25	0	0	0	0
Ba	0.69	0.76	0	0	0	0
Pb	0	0.11	0	0	0	0
Zr	0	0	0	0	0	1.01
Hf	0	0	0	0	0	0.01
Nb	0	0	0	0	0	0
Nd	0	0	0	0	0	0
U	0	0	0	0	0	0
F	0	0	0	0.08	0.02	0

* Data determined using WDS-mode analysis.

zolkin et al. 2016). The formula coefficient of Zn has been added to Mg+Fe *apfu* because Mg and Zn easily substitute each other in numerous minerals.

The calculated pressure range for the analysis corresponding to the first generation of phengites (Zn-rich celadonite inside of titanite crystals), is 24.7 to 22.6 kbar for the upper temperature limit of the crystallization of the rim of rutile grains. The crystallization of rutile fin-

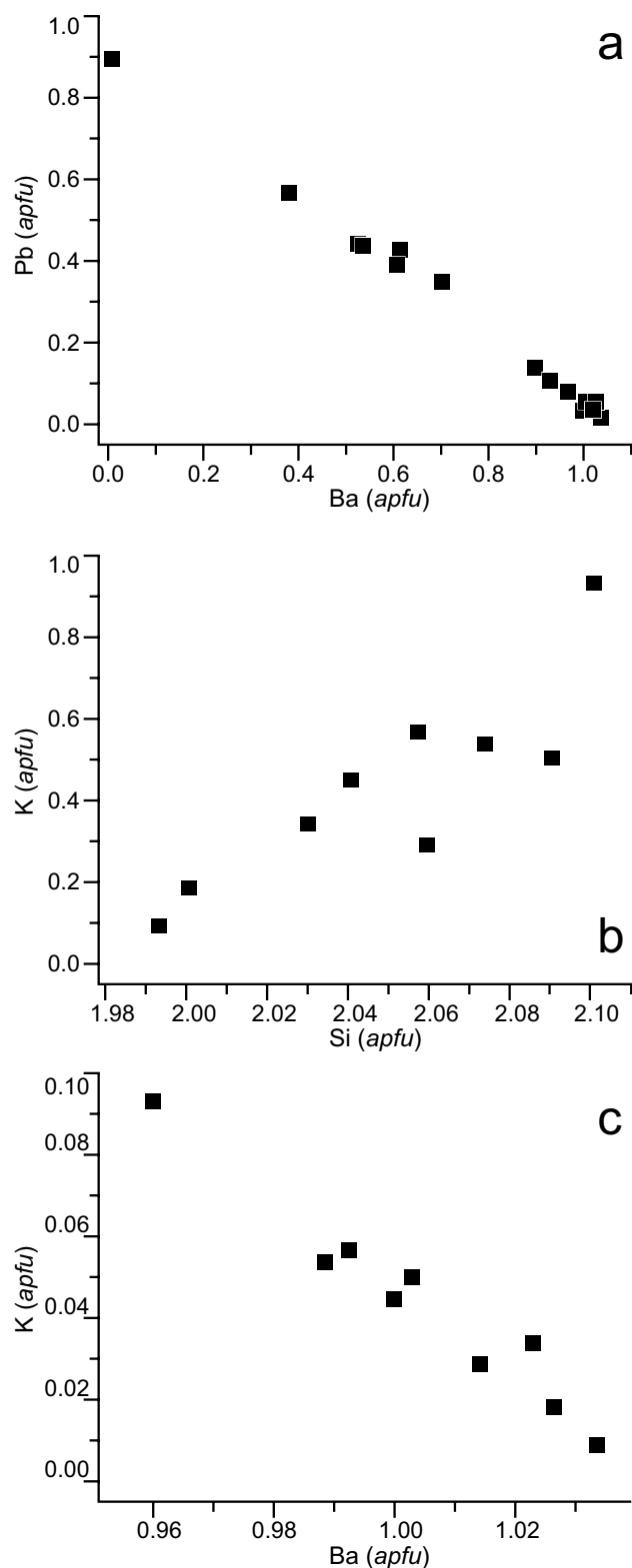


Fig. 4. **a** – Correlation between Ba and Pb contents in sulfates with the general formula $(\text{Ba,Pb})\text{SO}_4$. Correlation coefficient $R = -0.997$; **b** – Correlation between K and Si contents in cymrite (formula coefficients calculated on $\text{Al} + \text{Si} = 4$ apfu). Correlation coefficient $R = 0.863$; **c** – Correlation between K and Ba contents in cymrite (formula coefficients calculated on $\text{Al} + \text{Si} = 4$ apfu). Correlation coefficient $R = -0.976$.

ished at temperatures below 500°C and the upper limit of pressure estimated using Zn-rich phengite for this temperature is 22.8 kbar.

The calculated pressure ranges for the analyses corresponding to the second generation of phengites, are 7.1 to 4.0 kbar, respectively for temperatures between 450 and 350°C , *i.e.* at the stage preceding cymrite formation. This shows a significant decrease of pressure during the second stage of crystallization. This might imply that the described mineral assemblage formed during the third stage of formation of the Nežilovo occurrence (retrograde metamorphism) as suggested by Bermanec et al. (2021). Apart from the change in pressure, this might also be seen in the presence of high content of chalcophile elements which are considered to partially originate from post-magmatic fluids (Barić and Ivanov 1960; Chukanov et al. 2015; Ermolaeva et al. 2016).

Baryte and anglesite form solid-solution series which has gaps between ~ 0.1 – 0.4 and ~ 0.7 – 0.9 Ba apfu (Fig. 4a). The compositions without Ba correspond to anglesite of the second generation. First generation anglesite and second generation baryte constituting pseudomorphs after galena contain 0.4 – 0.7 or ~ 0.9 – 0.95 Ba apfu. The Pb-free BaSO_4 phase is a relic of baryte schist. Baryte–anglesite solid solution is incomplete, and the chemical zoning is observed in the samples (Fig. 2g). Consequently, the temperatures at which galena was substituted by Pb,Ba-sulfates was significantly lower than 750°C which would be required to obtain zoning-free BaSO_4 – PbSO_4 solid solution (Hsiu-Ru et al. 2002).

Based on data from the studied mineral paragenesis, one can distinguish at least four stages corresponding to different temperatures (Fig. 3). The estimated temperature interval for cores of rutile grains and titanite is between 535 and 613°C . The formation of outer zones of rutile grains, substitution of galena with sulfates, decomposition of sphalerite, formation of Zn-bearing and Ba-free mica occurred significantly below 600°C and probably even somewhat below 500°C . Zn-free and Ba-bearing mica and cymrite crystallized in the temperature interval between 350 and 500°C and below 350°C , respectively. Data on hydrothermal synthesis (Hsu 1994) showed that cymrite can be stable under hydrothermal near-surface conditions at a temperature somewhat higher than 250°C and under conditions of low-grade metamorphism corresponding to greenschist facies. Baryte solubility in neutral aqueous media below 300°C is very low, however, in alkaline medium transformation of baryte into cymrite by the reaction $\text{BaSO}_4 + 2\text{OH}^- + \text{Al}_2\text{O}_3 + 2\text{SiO}_2 \rightarrow \text{BaAl}_2\text{Si}_6\text{O}_8 \cdot \text{H}_2\text{O} + \text{SO}_4^{2-}$ occurs under low-temperature hydrothermal conditions (Hsu 1994). Thus, the estimated temperature interval of cymrite crystallization at the Kalugeri locality is 200 – 350°C . The presence of K and Na in cymrite from the Kalugeri locality indicates that it

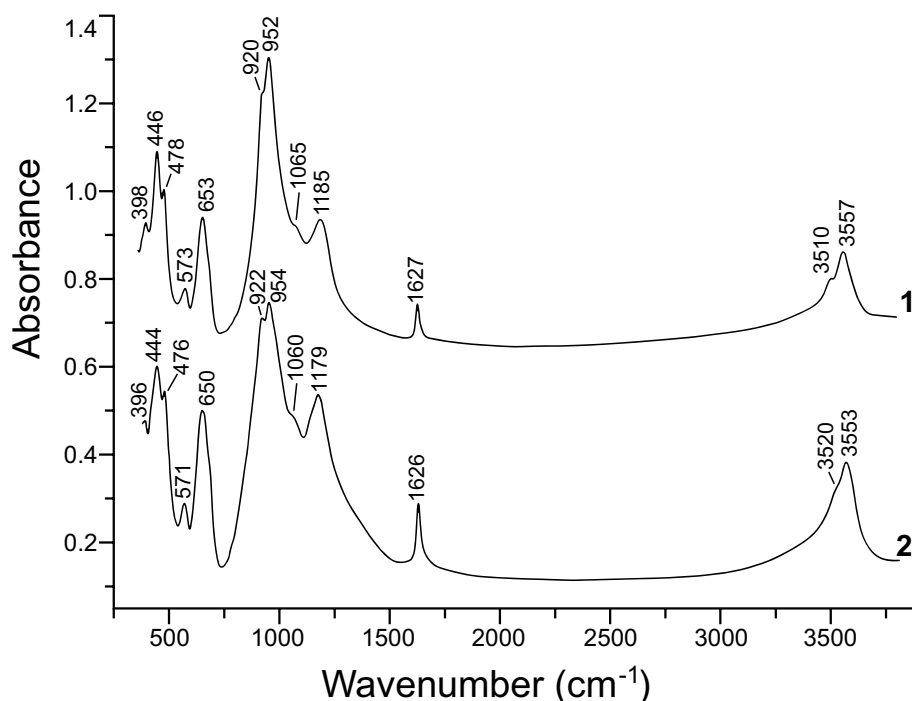


Fig. 5. IR spectra of (1) cymrite from Nežilovo (this work) and (2) monoclinic cymrite from a hydrothermal association with zeolites at the Kovdor phlogopite deposit, Kola Peninsula (Sorokhtina et al. 2008).

could have crystallized as a result of the reaction between baryte and alkaline hydrothermal solution (see Blount 1977; Zhen-Wu et al. 2014; Chukanov et al. 2020a, b).

A positive correlation between the formula coefficients of K and Si and negative correlation between those of K and Ba are observed for cymrite (Figs 4b, c) whereas significant (with $|R| > 0.5$) pair correlations involving Na, Ca and other admixed components are absent. Thus, the main scheme of isomorphism in cymrite from the Kalugeri locality is $Ba + Al \leftrightarrow K + Si$.

5. Conclusions

Regional metamorphosed metasomatic rocks of the Nežilovo area are usually characterized as microlocalities of complex ores with chalcophile elements occurring in oxides and oxysalts. However, an anomalous sulfide-bearing mineral assemblage has been discovered at the Kalugeri locality. Partial substitution of sulfides with oxygen-bearing minerals is observed which gives further insights into the complex history of formation of this locality. This shows that sulfide-free Nežilovo type ores might form as a result of transformation of initial sulfide ores at low-PT conditions and a high barium activity. At least four stages of the deposit formation can be distinguished based on mineral paragenesis and associations: between 535 and 613 °C (cores of rutile grains), about 500 °C and probably somewhat below 500 °C (outer zones of rutile grains, substitution of galena with sulfates, decomposition of sphalerite, formation of Zn-bearing and Ba-free mica), significantly lower than 500 °C but above

350 °C (crystallization of Zn-free and Ba-bearing mica) and below 350 °C (crystallization of cymrite). During the formation of the sulfide-bearing mineral assemblage at the Kalugeri locality, lowering of pressure from 22.6–24.7 to around 4 kbar took place.

Acknowledgements. Constructive comments of two anonymous reviewers are gratefully acknowledged. This work was performed in accordance with the state task, state registration No. AAAA-A19-119092390076-7.

References

- ARMBRUSTER T, BERMANEC V, ZEBEC V, OBERHÄNSLI R (1998) Titanium and iron poor zincohobomite-16H, $Zn_{14}(Al, Fe^{3+}, Ti, Mg)_8Al_{24}O_{62}(OH)_2$, from Nežilovo, Macedonia: Occurrence and crystal structure of a new polysome. *Schweiz Mineral Petrol Mitt* 78(3): 469–477
- BARIĆ LJ (1960) Piemontit, gahnit und rutil aus dem Fundort der Blei und Zinkerze bei dem Dorfe Nežilovo in Mazedonien. *Glas Prirodnac Muz Beograd Ser A* 13: 200–204 (in German)
- BARIĆ LJ, IVANOV T (1960) Mineralvergesellschaftung in der Umgebung des Dorfes Nežilovo am Jakupica Gebirge in Mazedonien. *Bull Sci A (Zagreb)* 5: 2 (in German)
- BERMANEC V, ARMBRUSTER T, OBERHÄNSLI R (1994) Crystal chemistry of Pb- and REE-rich piemontite from Nežilovo, Macedonia. *Schweiz Mineral Petrogr Mitt* 74: 321–328
- BERMANEC V, HOLTSTAM D, STURMAN D, CRIDDLE A, BACK M, ŠČAVNIČAR S (1996) Nežilovite, a new member of

- the magnetoplumbite group, and the crystal chemistry of magnetoplumbite and hibonite. *Canad Mineral* 34: 1287–1297
- BERMANEC M, CHUKANOV NV, BOEV I, ŠTURMAN BD, ZEBEC V, BERMANEC V (2021) Ardenite-bearing mineral association related to sulfide-free ores with chalcophile metals at Nežilovo, Pelagonian Massif, North Macedonia. *Eur J Mineral* 33: 433–445
- BLOUNT CW (1977) Barite solubilities and thermodynamic quantities up to 300 °C and 1400 bars. *Amer Miner* 62: 942–957
- BOEV I, BERMANEC M (2021) Geology, Petrology and the Age of Pegmatites in Alinci Locality (North Macedonia). *Nat Resour Technol* 15(2): 33–41
- CHUKANOV NV, VARLAMOV DA, NESTOLA F, BELAKOVSKIY DI, GOETTLICHER J, BRITVIN SN, LANZA A, JANČEV S (2012) Piemontite-(Pb), $\text{CaPbAl}_2\text{Mn}^{3+}[\text{Si}_2\text{O}_7][\text{SiO}_4]\text{O}(\text{OH})$, a new mineral species of the epidote supergroup. *Neu Jb Mineral, Abh* 189(3): 275–286
- CHUKANOV NV, JANČEV S, PEKOV IV (2015) The association of oxygen-bearing minerals of chalcophile elements in the orogenic zone related to the “Mixed Series” complex near Nežilovo, Republic of Macedonia. *Maced J Chem Chem Eng* 34: 115–124
- CHUKANOV NV, AKSENOV SM, JANČEV S, PEKOV IV, GÖTTLICHER J, POLEKHOVSKY YUS, RUSAKOV VS, NELYUBINA YUV, VAN KY (2016) A new mineral species ferricoronadite, $\text{Pb}[\text{Mn}_6^{4+}(\text{Fe}^{3+}, \text{Mn}^{3+})_2]\text{O}_{16}$: mineralogical characterization, crystal chemistry and physical properties. *Phys Chem Miner* 43: 503–514
- CHUKANOV NV, ZUBKOVA NV, SCHÄFER C, VARLAMOV DA, ERMOLAeva VN, POLEKHOVSKY YUS, JANČEV S, PEKOV IV, PUSHCHAROVSKY DYU (2018a) New data on ferriakasakaite-(La) and related minerals extending the compositional field of the epidote supergroup. *Eur J Mineral* 30: 323–332
- CHUKANOV NV, KRZHIZHANOVSKAYA MG, JANČEV S, PEKOV IV, VARLAMOV DA, GÖTTLICHER J, RUSAKOV VS, POLEKHOVSKY YUS, CHERVONNYI AD, ERMOLAeva VN (2018b) Zincovelesite-6N6S, $\text{Zn}_3(\text{Fe}^{3+}, \text{Mn}^{3+}, \text{Al}, \text{Ti})_8\text{O}_{15}(\text{OH})$, a new högbomite-super group mineral from Jakupica mountains, Republic of Macedonia. *Mineral Petrol* 112: 733–742
- CHUKANOV NV, VOROBEI SS, ERMOLAeva VN, VARLAMOV DA, PLECHOV PY, JANČEV S, BOVKUN AV (2019) New data on chemical composition and vibrational spectra of magnetoplumbite-group minerals. *Geol Ore Depos* 61: 637–646
- CHUKANOV NV, VARLAMOV DA, ERMOLAeva VN, JANČEV S (2020a) The role of barium in the formation of sulfide-free ores with chalcophile elements in the “Mixed Series” of the Pelagonian Massif. *Proc Rus Mineral Soc* 149(1): 96–107
- CHUKANOV NV, ZUBKOVA NV, JANČEV S, PEKOV IV, ERMOLAeva VN, VARLAMOV DA, BELAKOVSKIY DI, BRITVIN SN (2020b) Zinc-rich and copper-bearing amphiboles from sulfide-free ore occurrences of the Pelagonian massif, Republic of North Macedonia. *Mineral Petrol* 114: 129–140
- DUNN PJ (1991) Rare minerals of the Kombat Mine. *Mineral Rec* 22: 421–425
- ERMOLAeva VN, CHUKANOV NV, JANČEV S, VAN K (2016) Endogenic oxide parageneses with chalcophile elements in the orogenic zone related to the “Mixed Series” of the Pelagonian massif, Republic of Macedonia. *New Data on Minerals* 51: 12–19
- ERMOLAeva VN, VARLAMOV DA, CHUKANOV NV, JANČEV S (2019a) Forms of arsenic concentration in sulfide-free endogenous Pb–Zn–Sb ores of the Pelagonian massif, Republic of North Macedonia. *Geol Ore Depos* 61: 782–790
- ERMOLAeva VN, VARLAMOV DA, JANČEV S, CHUKANOV NV (2019b) Spinel- and högbomite-super group minerals from sulfide-free endogenic Pb–Zn–Sb–As assemblage in Pelagonian Massif, Republic of North Macedonia. *Geol Ore Depos* 61(7): 1–9
- HOLTSTAM D, GATEDAL K, SÖDERSBERG K, NORRESTAM R (2001) Rinmanite, $\text{Zn}_2\text{Sb}_2\text{Mg}_2\text{Fe}_4\text{O}_{14}(\text{OH})_2$, a new mineral species with a nolanite-type structure from the Garpenberg Norra mine, Dalarna, Sweden. *Canad Mineral* 39: 1675–1683
- HSIU-RU W, JIANN-SHING L, SHU-CHENG Y (2002) Synthesis of zoning-free BaSO_4 – PbSO_4 solid solution and its structural characterizations. *Z Kristallogr* 317: 143–148
- Hsu LS (1994) Cymrite: new occurrence and stability. *Contrib Mineral Petrol* 118: 314–320
- INNES J, CHAPLIN RC (1986) Ore bodies of the Kombat mine, South West Africa/Namibia. In: ANHEUSSER C R, MASKE S (eds) *Mineral deposits of southern Africa*. Geological Society of South Africa, pp 1789–1805
- IVANOV T (1961) Geological report on the investigations of the ore occurrences at the Nezilovo village. Geological Survey Institute, Skopje, Republic of Macedonia. pp 45 (in Macedonian)
- IVANOV T, JANČEV S (1976) “Nežilovo” – a complex polymetallic deposit of “Franklin Furnace” type in Macedonia. *Proceedings of the Yugoslavian Geological Congress 5*, Ljubljana, 1976, pp 69–78
- JANČEV S (1975a) Development of a mixed series in the pre-cambrian complex of the Pelagonian massif in the upper part of the river Babuna, Macedonia. *Bull Sci A (Zagreb)* 20: 275–276
- JANČEV S (1975b) Ore occurrence of cymrite at the village of Nezilovo in Macedonia. *Bull Sci A (Zagreb)* 20: 9–10
- JANČEV S (1984) A mineral of hedyphane $(\text{Pb}, \text{Ca})_5(\text{AsO}_4)_3\text{Cl}$ structure from “the mixed series” in the upper part of the Babuna river, Macedonia. *Geol Maced* 1(1): 57–61
- JANČEV S (1994) Ba-rich and Zn-rich silicate minerals, Sb-rich gahnite and braunite from the ore occurrences in the

- mixed series of the Pelagonian massif at the village of Nežilovo in Macedonia. *Geol Maced* 8(1): 39–44
- JANČEV S (1998) Zn-rich pyroxenes from the occurrences in the mixed series the upper part of the Babuna River, Macedonia. *Geologija (Ljubljana)* 40: 283–289
- JANČEV S, CHUKANOV NV, ERMOLAEVA VN (2016) Association of oxide minerals-concentrators of chalcophile elements (Pb, Zn, Sb) from the “Mixed Series” near Nežilovo village, Macedonia. In: *Materials of the Third Congress of Geologists of Republic of Macedonia, Struga, 2016(2)*: 401–404
- JANČEV S, CHUKANOV NV, VARLAMOV DA, ERMOLAEVA VN (2021) New and potentially new minerals of the hogbömite and spinel supergroups from the ore occurrences at the Nežilovo village, Veles municipality, North Macedonia. *J. nat. sci. math. of UT* 6(11–12): 31–39
- KAMZOLKIN VA, IVANOV SD, KONILOV AN (2016) Empirical phengite geobarometer: Background, calibration, and application. *Geol Ore Depos* 58: 613–622
- MAJER V, MASON R (1983) High-pressure metamorphism between the Pelagonian Massif and Vardar Ophiolite Belt, Yugoslavia. *Mineral Mag* 47: 139–141
- MOST T (2003) Geodynamic evolution of the Eastern Pelagonian Zone in northwestern Greece and the Republic of Macedonia, Implications from U/Pb, Rb/Sr, K/Ar, $^{40}\text{Ar}/^{39}\text{Ar}$ geochronology and fission track thermochronology. PhD thesis, Geowissenschaftliche Fakultät der Eberhardt-Karls-Universität, Tübingen, Germany, 98
- MOUNTRAKIS D (1984) Structural evolution of the Pelagonian Zone in Northwestern Macedonia, Greece. *Geological Society Special Publication, London*, 17: 581–590
- NYSTEN P, HOLTSTAM D, JONSSON E (1999) The Långban minerals. In: HOLTSTAM D, LANGHOF J (eds) *Långban: The mines, their minerals, geology and explorers*. Raster Förlag and the Swedish Museum of Natural History, pp 89–183
- PALACHE C (1929a) A comparison of the ore deposits of Långban, Sweden, with those of Franklin, New Jersey. *Amer Miner* 14(2): 43–47
- PALACHE C (1929b) Paragenetic classification of the minerals of Franklin, New Jersey. *Amer Miner* 14(1): 1–18
- PALACHE C (1937) *The minerals of Franklin and Sterling Hill, Sussex County, New Jersey*. US Government Printing Office, Washington, pp 1–161
- PECK WH, VOLKERT RA, MANSUR AT, DOVERSPIKE BA (2009) Stable isotope and petrologic evidence for the origin of regional marble-hosted magnetite deposits and the zinc deposits at Franklin and Sterling Hill, New Jersey Highlands, United States. *Econ Geol* 104: 1037–1054
- SOROKHTINA NV, CHUKANOV NV, VOLOSHIN AV, PAKHOVSKY YAA, BOGDANOV AN, MOISEEV MM (2008) Cymrite as an indicator of high barium activity in the formation of hydrothermal rocks related to carbonatites of the Kola Peninsula. *Geol Ore Depos* 50(7): 620–628
- STOJANOV R (1960) Geological and petrographical composition of the central part of the Pelagonian metamorphic massif. *Trudovi na Geoloskiot Zavod na Narodna Republika Makedonija* 7: 147–180 (in Macedonian)
- STOJANOV R (1968) Phengites of the Pelagonian massif. *Trud Geol Zav Socijal Republ Makedonija*, 13, 59–73 (in Macedonian)
- TARR WA (1929) The origin of the zink deposits at Franklin and Sterling Hill, New Jersey. *Amer Miner* 14: 207–221
- TURNER RW, RUMSEY MS (2010) Mineral relationships in the Mendip Hills. *J Russell Soc* 13: 3–47
- VARLAMOV DA, ERMOLAEVA VN, JANČEV S, CHUKANOV NV (2018) Oxides of the pyrochlore supergroup from a nonsulfide endogenic assemblage of Pb–Zn–Sb–As minerals in the Pelagonian massif, Macedonia. *Geol Ore Depos* 60(8): 717–725
- VARLAMOV DA, ERMOLAEVA VN, CHUKANOV NV, JANČEV S, VIGASINA MF, PLECHOV PYU (2019) New data on epidote-supergroup minerals: unusual chemical compositions, typochemistry, and Raman spectroscopy. *Geol Ore Depos* 61:827–842
- VARLAMOV DA, ERMOLAEVA VN, CHUKANOV NV, JANČEV S (2021) Mineralogy of copper in sulfide-free Pb–Zn–Sb ores of the Pelagonian massif, Republic of North Macedonia. *Proc Rus Mineral Soc* 150(4): 103–114 (in Russian)
- WARR LN (2021) IMA–CNMNC approved mineral symbols. *Mineral Mag* 85(3): 291–320
- WATSON EB, WARK DA, THOMAS JB (2006) Crystallization thermometers for zircon and rutile. *Contrib Mineral Petrol* 151: 413–433
- WILKERSON AS (1962) *The minerals of Franklin and Sterling Hill, New Jersey*. Bulletin 65, New Jersey Geological Survey. Department of Conservation and Economic Development. Trenton, New Jersey, pp 1–80
- ZHEN-WU BY, DIDERIKSEN K, BELOVA DA, RAAHAUGE PJ, STIPP SLS (2014) A comparison of standard thermodynamic properties and solubility data for baryte, $\text{Ba}^{2+}(\text{aq})$ and $\text{SO}_4^{2-}(\text{aq})$. *Mineral Mag* 78: 1505–1515